J. Fluid Mech. (1980), *vol.* 96, *part* 2, *pp.* 287–297
Printed in Great Britain

The nonlinear capillary instability of a liquid jet. Part 3. Experiments on satellite drop formation and control

By K. C. CHAUDHARY
International Business Machines Corporation, General Products Division, San Jose, California
AND T. MAXWORTHY
Departments of Mechanical and Aerospace Engineering, University of Southern California, Los Angeles, California

(Received 30 June 1978 and in revised form 15 May 1979)

We continue the experiments of Chaudhary & Maxworthy (1980) to include the behaviour at and beyond the point along the jet at which individual drops interspersed with small satellite drops begin to form. In particular, we show how the perturbation wavenumber and amplitude for a fundamental disturbance alone combine to give a variety of modes of breakup into drops and a variety of patterns of drop recombination further downstream. We then show how the addition of a third harmonic to this fundamental can be used in a variety of parameter combinations to control the behaviour of the satellite drops and in some cases eliminate them completely.

1. Introduction

In recent years the capillary jet has been used in many practical applications such as printing (Sweet 1964), particle sorting (Herzenberg, Sweet & Herzenberg 1976), pelletizing, dispersing liquids, spinning of synthetic fibres, fuel injection, hydraulic mining, machining, etc. For the present work the most significant of these are printing and particle sorting where, for high fidelity operation, it is necessary to have a synchronized column of drops of precisely the same size and shape.

Previous nonlinear theory (Yuen 1968; Chaudhary 1977) and experimentsl work (Donnelly & Glaberson 1966; Goedde & Yuen 1970; Ruthland & Jameson 1970) on the capillary jet shows that in the synchronized breakup of the jet, large main drops are interspersed with smaller 'satellite' drops. In most applications, it is necessary to charge the drops individually in order to achieve varying amounts of deflexion. (A typical scheme for such an application being shown in figure 1.) Usually the presence of a satellite can defeat this purpose. Such a satellite can usually form in two distinct ways [see figure 2, (plate 1)]: (i) the main drop and satellite may detach from the main stream separately (figure 2*a*, *b*), in which case they will carry individual charges depending on their shape and size at the time of separation from the main stream (and the field produced by the charging device); and (ii) a ligament of liquid equal to one wavelength may detach from the main stream at one time and subsequently may divide itself into a main drop and one or more satellites (figure 2*c*). As the column

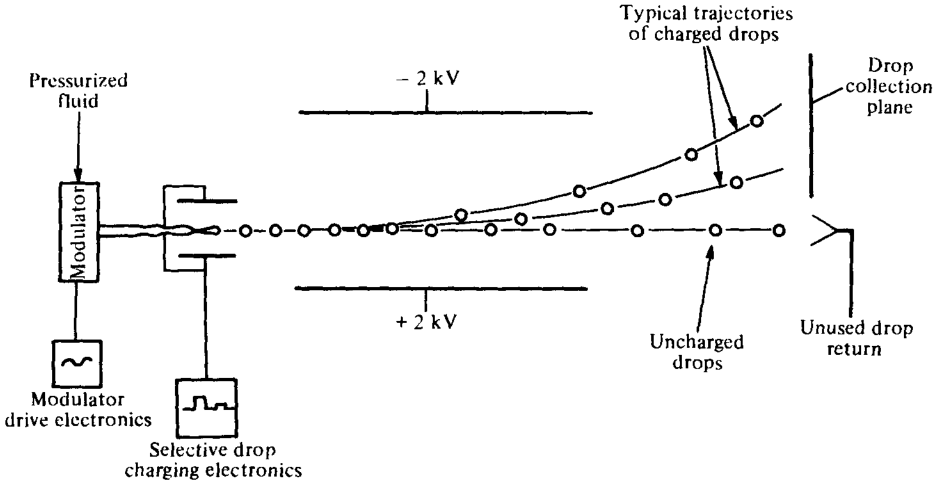

FIGURE 1. Schematic diagram of a typical jet deflexion apparatus, such as used in a printing application.

proceeds further down the stream there are two possibilities: (*a*) the satellite(s) may remain interspersed between the main drops ('no merging' or 'infinite satellite condition'), or (*b*) the satellite(s) may merge with the leading ('forward merging') or the following drop ('rearward merging').

The presence of satellites will be detrimental to the production of the desired end results in the following ways.

(i) If the satellites do not merge with the main drop before they are under the influence of the deflecting field, they will follow much steeper deflexion trajectories due to their larger charge-to-mass ratio, and will spoil the fidelity of the system or will deposit on the deflexion structure.

(ii) If the satellites do not merge with their parent drop, they will create an erroneous charge on the drop with which they do merge.

In general, it is most desirable to have no satellites at all. The presence of satellites may not be harmful if one whole wavelength of liquid separates from the main stream as a single unit. If satellites then do separate out, they must later merge with the same parent drop before being influenced by the deflecting field.

The work reported in this paper is motivated by the need to eliminate or at least achieve a favourable configuration for satellites in a liquid jet. All previous theoretical, as well as experimental, work has been aimed at an understanding of the breakup of a liquid column with a monochromatic applied disturbance and the presence of the satellites has been found to be a dominant feature. Therefore, we reasoned that by applying a non-monochromatic (a fundamental and one harmonic) disturbance a more desirable configuration of drops would be achieved. Chaudhary & Redekopp (1979) have developed a third-order solution for an initial velocity input (consisting of a fundamental and an arbitrary harmonic component) to the capillary jet. It was shown that, by including this harmonic component, the phase of the second harmonic could be made time dependent and could be varied in relation to the phase of the fundamental. This provided a suitable mechanism to control the satellite formation. The size and shape of the satellites (and of the main drops) depends on the initial conditions imposed, i.e. on the wavenumber (k_0), the magnitudes of the fundamental (ϵ) and the harmonic (δ_n) inputs and the phase (θ) of the harmonic in relation to the fundamental. It is difficult to derive analytical expressions for the size and shape of the satellites and the main drop, but one can carry out the solution for the progressive jet until the breakup point and then observe their size and the shape just before they detach sequentially from the main stream.

The theoretical solution gives no direct information on the dynamics of drops beyond the breakup because the radius of the jet becomes negative. Also if a long ligament breaks from the main stream (figure 2*c*), the solution does not give any information as to whether or not there will be subsequent breakup of the ligament to give satellites.

In this paper we study experimentally the characteristics and control of these satellites. In § 2 the mechanism for the merging of the satellites with the main drops is explained. In § 3.1 we investigate the characteristics of the satellites with the fundamental input alone. In § 3.2 the effect of a (third) harmonic input on the direction of merging of the satellites is discussed; in § 3.3 control and elimination of satellites is investigated.

The apparatus used in the present investigation has been described (Chaudhary & Maxworthy 1980) and that description need not be repeated here.

2. Comments on the mechanism of satellite merging

Once a drop or a satellite is detached from the main stream, it becomes an isolated mass of fluid suspended in space (in a vacuum with no gravity as assumed in the formulation of the problem). Any subsequent motion of this isolated mass should depend primarily on the surface tension forces and the axial momentum (or velocity) distribution at the instant of breakoff from the main stream. The velocity distribution at the instant of breakoff and the subsequent accelerations created by the surface tension force give an oscillatory motion to this isolated mass until it eventually becomes spherical as these velocities decay due to viscous dissipation.

Figure 2 shows how the satellites and the main drop become elongated alternately in the radial and axial directions Depending on how the perturbation velocities are distributed at the instant of breakup, these isolated masses (i.e. the main drop or the satellite) can have a different velocity in the z (or axial direction) compared to the mean axial velocity of the progressive jet. This difference in axial velocity of a main drop and a satellite can cause them to merge together further downstream and, if this difference is large enough, they can merge even before the oscillations have died down. Thus, it is the perturbation momentum (or equivalently the axial perturbation velocity distribution) at the instant of the breakoff which decides the direction of merging of the satellites.

3. Results

3.1. *Satellite characteristics with fundamental input only*

By examining all three orders of the solution (Chaudhary & Redekopp 1980), for the case of a fundamental input only, one observes that all the harmonic components ($\cos 2k\zeta$, $\cos 3k\zeta$ terms) are in phase with the fundamental ($\cos k\zeta$). One may then conjecture that, with fundamental input alone, if a satellite does in fact form, it will perhaps remain interspersed between main drops or will merge only after travelling far along the z axis. One may also conjecture that changing the magnitude of the fundamental input (ϵ) will not affect the direction of merging, since all the harmonics always remain in phase with the fundamental. However, as described in the previous section, the theory is not able to predict the droplet behaviour unambiguously and we must rely eventually on the experimental results to determine the correct sequence of events.

Some numerical calculations were performed with a fundamental input alone. In those cases with moderate wavelength, it was observed that the crest of the satellite and the crest of the main drop were always spaced one-half wavelength apart. This indicates that the second harmonic component is mainly responsible for the formation of the satellites in the range of moderate wavelengths. With long wavelengths the possibility of the formation of two satellites exists, while with short wavelengths, the solution shows there may not be any satellites even with the fundamental input alone. Some of these theoretical results are shown in figures 2, 3 and 4 of Chaudhary & Redekopp (1980).

Experiments were performed to investigate the general formation and merging characteristics of the satellites. In all of these a fundamental input of 100 kHz was used. In general, it was found that with a low modulator drive-voltage the satellites merged in the rear direction a short time after breakoff. As the drive voltage was increased, the time (or equivalently the distance) of merging of the satellites increased. At a certain voltage (V_∞), the 'no-merge' condition was reached. This voltage (V_∞) was dependent on the wavenumber. With drive voltage greater than V_∞, the satellites merged in the forward direction.

Figure 3 shows the general merging characteristics of the satellites, where non-dimensional merge time is plotted against the ratio of drive voltage V_e to the no-merge condition voltage V_∞. It can be observed that, as the wavenumber is increased from 0·31 to 0·61, the satellites merge in a shorter time in both the rear and forward directions. Additionally, figure 4 shows the relation between the wavenumber and the V_∞ voltage.

An attempt was made to determine experimentally whether the mode of drop separation from the jet (i.e. either the rear-separation or the forward-separation conditions†) had any relationship to the mode of merging of the satellites. No clear-cut correlation could be found. As already noted it was observed that forward separation occurs for low drive voltage, and rear separation occurs for high drive voltage, and at the transition the forward and rear separations occur at the same point along the z axis. For the four values of the wavenumber used in figure 3, the transition occurs at the following values (see figure 3).

k_0 ...	0·31	0·4312	0·51	0·61
V_e/V_∞ at transition	0·682	0·442	0·366	0·678

Clearly, there is no clear correlation between the two types of separation and the two types of merging condition.

† If the jet is observed at the instant when the breakup point is at a minimum distance from the nozzle and if a satellite drop has just separated from the jet, the condition is called 'rear separation' of the satellite (or just 'rear separation') (see figures 2*b*, *c*, 9*c*). On the other hand, if a main drop has just separated, it is called 'forward separation' (see figures 2*a*, 9*f*, 12*d*).

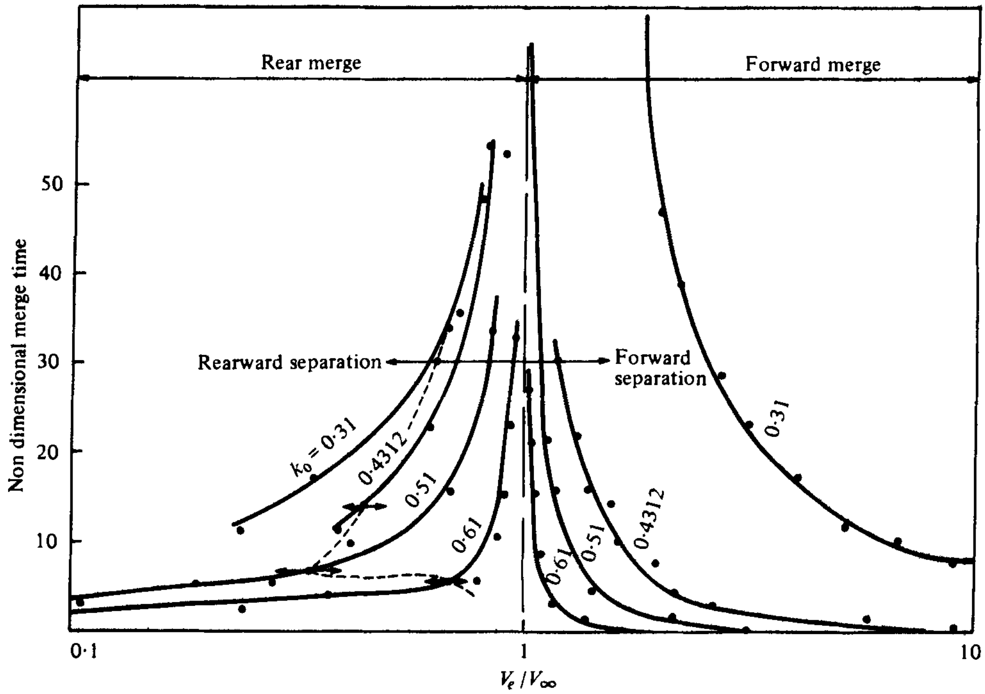

FIGURE 3. Merging characteristics of satellites for fundamental input only at various wavenumbers. V_c = fundamental drive voltage; V_∞ = voltage for no-merge condition.

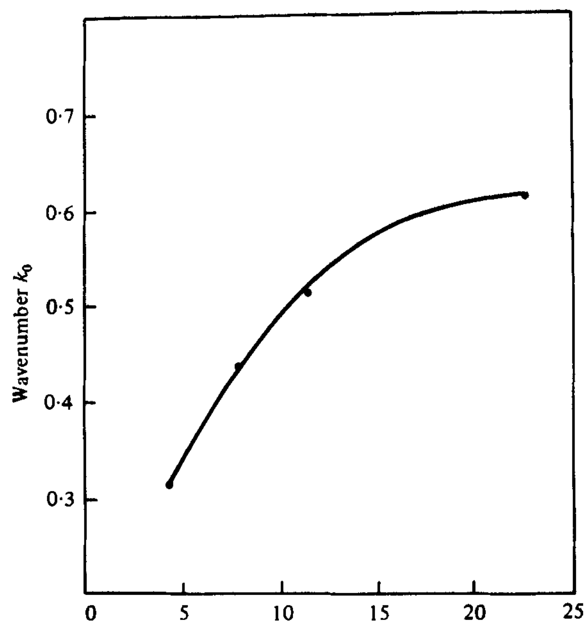

FIGURE 4. Fundamental input voltage for no-merge condition (V_∞) as a function of wavenumber.

3.2. *Experiments on the direction of satellite merging with harmonic input*

A set of experiments was performed to determine the effect of the phase angle θ of the third harmonic input on satellite merging. For these experiments k_0 was selected to be equal to 0·4312 and the fundamental input was set at 100 kHz. Since it is possible that the modulator generates some harmonics even with a pure fundamental input, the following technique was used to reduce the effect of these harmonics. The drive voltage of the fundamental input (with no harmonic applied) was adjusted to give the satellite 'no-merging' condition, in this case 8·8 V r.m.s. (see figure 4). With the fundamental set at this value, we assume that when the harmonic is applied along with the fundamental any merging of the satellites should be due to the harmonic only.

The third harmonic input voltage was set at 2·2 V r.m.s. (i.e. 25 % of the fundamental) and the phase angle θ of the harmonic was changed in steps of $-45°$, from $\theta = 0$ to $\theta = -315°$. Figure 5 (plate 2) shows the experimental jet profiles near the breakoff point, for these experiments, including the profile for no harmonic input. The figure shows that after a certain number of wavelengths, the satellites merge; the direction of merging is also shown. It is observed from these experiments that, as θ is changed over 360°, the satellites merging completes one full cycle of behaviour. From figure 5(*c*) and (*d*) ($\theta = -45°$ and $-90°$), the satellite changes from forward merging to rear merging, implying that in between there was a no-merging condition. As θ is reduced further, first there is more rapid rear merging and then a further no-merging condition exists between $\theta = -225°$ and $-270°$. Then a fast forward-merging condition is found and again a no-merge condition at the end of the cycle. Thus, there are two no-merge conditions 180° apart, which separate the two forward- and rear-merging zones. This clearly demonstrates that the direction of the satellite merging can be controlled with the (third) harmonic input.

Calculations of perturbation momentum were not carried out to correlate these results to a possible theoretical prediction. However, several computer runs were made with different amounts of third harmonic input, to find if there was any relative axial movements between the crest (and/or neck) of the satellite and the crest (and/or neck) of the main drop. It was thought that, if such a relative movement between the two crests (of a satellite and an adjacent drop) could be observed from the numerical values of the jet profile, some easy correlation between direction of merging and theoretical movement of these crests could be found. Unfortunately, no such correlation was found because in the theoretical jet profile the crest of the satellite was always one-half wavelength away from the crest of the main drop.

3.3 *Satellite control and elimination*

The primary purpose of the present work was to eliminate or to control the behaviour of satellites of a capillary jet of small diameter. At the outset it was thought that the inclusion of a harmonic with appropriate initial conditions with respect to the fundamental should lead to such a desired control. After much experimental work and theoretical computations, a large range of parameters was found which gave the desired behaviour of the satellites. All of the results presented here are for the case where only the third harmonic was included, but we realize that it may be possible to achieve equivalent results with a different choice of harmonic.

The fundamental input was kept at 100 kHz, at which the jet modulator charac-

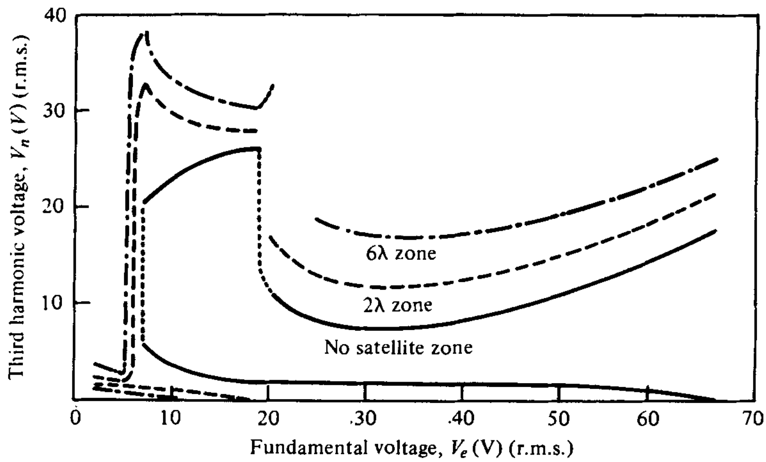

FIGURE 6. Satellite control diagram with third harmonic. $k_0 = 0{\cdot}4312$. Phase of the harmonic $\theta = 0°$. Satellite zones shown are for acceptable configurations. ——, no satellite zone; – – –, satellite merges in less than 2λ; —·—, satellite merges in less than 6λ.

teristics were already known (Chaudhary & Maxworthy 1980). Thus the third harmonic was 30 kHz, with the following parameters left free for the control of satellites:

k_0 = the wavenumber of the fundamental,

V_e, ϵ = the initial magnitudes of the drive voltage and input of the fundamental disturbance,

V_n, δ_n = the initial magnitudes of the drive voltage and input of the (third) harmonic disturbance,

θ = the phase of the (third) harmonic with respect to the fundamental.

During the course of preliminary experiments, it was found that having the third harmonic in phase with the fundamental gave the most effective control (and elimination) of satellites. Changing the phase from slightly leading to slightly lagging (in steps of $\frac{1}{16}$ of a cycle) changed the behaviour of the satellites in a gradual manner, indicating that the operation was in a stable parameter range rather than at an isolated unstable point. Only in a limited range of non-dimensional wavenumber, $0{\cdot}34 < k_0 < 0{\cdot}060$, was the control of the satellite effective, while the best results were in the neighbourhood of $k_0 = 0{\cdot}4312$. Again in this range of wavenumbers, the behaviour of satellites varied smoothly.

(*a*) *Satellite control at the most favourable wavenumber for 3rd harmonic input.* Figure 6 shows the pattern of satellites behaviour at $k_0 = 0{\cdot}4312$, which approximates the wavenumber for the best control with the third harmonic. The two axes represent the fundamental (100 kHz) and the third harmonic (300 kHz) voltages, with the harmonic in phase with fundamental. The region within the solid lines represents, for a given V_e, the range of V_n for which no satellite exists. The other two lines represent the range of V_n where satellites exist but have an acceptable configuration. The broken line represents the range of V_n where the satellite(s) merged with the parent drop within at most two wavelengths (2λ) of breakoff. The chain dotted line represents the range of V_n where the satellite(s) merged with the parent drop within at most six wavelengths (6λ) after the breakoff. In all these experiments the satellite merged in the forward direction. Several features should be noted:

(i) For low initial input ($V_e \leqslant 7$ V r.m.s.), the satellites cannot be eliminated. The harmonic simply helps to reduce the distance within which the satellites merge and brings the break point towards the rearward direction so that the satellites merge with the parent drop giving an acceptable satellite control.

(ii) At $V_e = 7$, there is large range of V_n where satellites can be eliminated.

(iii) In the range $7 \leqslant V_e \leqslant 18{\cdot}5$, there is a gradual increase in the range where satellites can be eliminated and consequently there are also large ranges for the other two curves. In this range, as V_e is increased, the lower curves for the 2λ and the 6λ merging zones go to zero harmonic level.

(iv) At about $V_e = 18{\cdot}5$, there is a large discontinuity. As the harmonic voltage V_n is increased from zero, first the satellites are eliminated. This represents the continuance of the lower solid line. However, as V_n is increased further, there is a change in the pattern of satellite formation. Figure 7 (plate 3) shows how the pattern of satellite formation changes (from a large satellite separating at the forward neck to a small satellite formed from a thin ligament) as the fundamental drive is increased from 18·5 to 20 V. This long ligament of fluid, which was coalescing with fluid ahead for low V_e, starts to break up and gives a small satellite. Therefore, the range in which the satellites can be eliminated is reduced. Consequently, there is discontinuity in the 2λ curve also. These small satellites merge quickly with the parent drop and the pattern of the 6λ curve does not change till the fundamental drive is increased to 22 V. Since the dynamics of such a jet are very nonlinear, discontinuities in the satellite pattern should be expected. Actually, what is being measured in this case is a discrete quantity (the number of satellites in any pattern) from a continuous phenomenon. The long ligament starts to develop a neck of its own at some value of V_e but it then contracts rapidly into the main drop and the small satellite does not separate out. However, for large V_e this neck develops so rapidly that it breaks off before the ligament can coalesce with the main drop. Thus, the formation of the small satellite is a result of gradual change in the pattern of filament development, but observing only the single point where it separates out gives discontinuities in the curves.

(v) All curves beyond $V_e = 20$ V represent uniform gradual changes. At very large fundamental driving amplitudes ($V_e = 66$ V), there are no satellites even without the harmonic input. Perhaps this is due to the effect of the particular jet modulator being used, since for large fundamental inputs it may not produce a pure initial disturbance and the distortion introduced by the modulator is of such a nature that satellites are eliminated.

Also, it was observed that at the discontinuity described above the operation is not very stable to changes in θ. A small change in this phase angle of the harmonic with respect to the fundamental changed the point of discontinuity. In particular, the formation of the small satellite could be delayed, showing that at such a discontinuity the third harmonic is not necessarily most effective when in phase with the fundamental.

Figures 8–10 (plates 4–6) show some typical modes of formation of satellites and the jet profile in the neighbourhood of breakup for some selected values of V_e and V_n. The fundamental wavenumber in all of these figures in 0·4312.

Figure 8 shows that with low fundamental drive the configuration is unacceptable (figure 8a). With the inclusion of a small amount of the third harmonic, satellites form but the configuration becomes acceptable (figure 8*b*). When the phase (θ) of the harmonic is changed within $\pm 45°$, the configuration still stays acceptable (figures 8*c*, *d*) showing that a wide margin of phase is available for stable operation.

Figure 9 shows the results at $V_e = 17{\cdot}7$ V, which is slightly below the discontinuity voltage mentioned in figure 6. Here, even with no harmonic, the configuration is acceptable (figure 9*a*), but inclusion of the harmonic improves the configuration (figure 9*b*) and by changing the magnitude and phase the satellites can be eliminated (figures 9*c*, *g*). Again a wide margin of phase ($\theta = -135°$ to $+90°$) is available where the configuration stays acceptable (figures 9*d*, *e*). Figure 9(*f*) shows that, by changing the phase of the harmonic by 180°, the shape of the formation is reversed, indicating conclusively that control is due to the included harmonic. This reverse configuration is acceptable since there is no satellite.

Figure 10 shows results beyond the discontinuity points mentioned in figure 6. The jet configuration is acceptable even without harmonic input; however, inclusion of harmonics improves the formation and can eliminate the satellites. The satellites are formed from the breakup of the thin ligament, which was mentioned as the cause of the discontinuity in the curves of figure 6.

(*b*) *Satellite control at other wavenumbers.* Figures 11–13 (plates 7–9) show some typical modes of satellite formation for other values of k_0, where control with the 3rd harmonic is also possible.

In figure 11, $k_0 = 0{\cdot}335$, which is approximately the lowest value of the wavenumber at which drop formation can be favourably controlled with the third harmonic. Due to the longer wavelength in this case, the ligament always breaks into satellites before coalescing with the drop. With fairly large fundamental drive voltages, small values of harmonic input move the crest of the satellite in the forward direction such that an acceptable configuration is possible.

In figure 12, where $k_0 = 0{\cdot}337$, the wavelength is still so long that complete elimination of satellites is not possible. However, from fairly low to fairly high values of the fundamental drive voltage, inclusion of the third harmonic results in an acceptable configuration. At $V_n = 3{\cdot}5$, the phase angle θ must be $+90°$ to give a forward-merging configuration. Changing the phase to $-90°$ reverses the shape of the formation (figure 12*d*).

In figure 13, $k_0 = 0{\cdot}604$, which is close to the highest value of fundamental wavenumber at which effective control with the third harmonic is possible. Here, the wavelength is small but there is a tendency to form a thin ligament which breaks easily into satellites. With high enough values of the fundamental and harmonic, it is possible to eliminate these satellites, but the phase angle needs to be different from zero.

4. Discussion and comparison with theory

It was found, while characterizing the modulator (Chaudhary & Maxworthy 1980), that the experimental and theoretical jet profiles did not match for the higher fundamental inputs. In comparing these to the various profiles presented below, it becomes evident that perhaps the modulator generates its own third harmonic (along with some other harmonics) even when only a fundamental input is applied.

(i) For example, in figure 14, we compare the profiles (*a*) and (*b*), with no harmonic input, to profiles (*c*), (*d*) and (*e*), with such an input. Although the breakup distances (not shown in the figure) were different for different fundamental inputs, the profiles near the breakup have a similar shape, showing that profiles for the higher fundamental inputs alone are similar to those with lower fundamental inputs with a small third harmonic.

(ii) In figure 15, the profiles (*a*), (*b*) and (*c*) are similar, indicating that there is a trade-off between the fundamental and the third harmonic inputs. Lower fundamental with higher 3rd harmonic input gives similar results as the higher fundamental with the lower 3rd harmonic input.

(iii) In figure 16, comparing the profile (*a*) with (*b*) to (*e*) shows that, when the no-satellite condition is obtained with fundamental input alone, the profile is similar to the profiles at lower fundamental inputs with the inclusion of sufficient third harmonic.

From a study of the above-mentioned profiles, it becomes evident that, in general, an acceptable configuration is best achieved with forward merging satellites. Further, both for the acceptable and no-satellite configurations, the jet profile in the neighbourhood of the breakup should develop in a 'carrot' shape (see figures 14–16, plates 10–12), i.e. with one neck in the rear direction and a gradual rise of the profile to the crest of the main drop.

The harmonics generated by the modulator itself, though helpful in giving an acceptable configuration, make it very difficult to compare these experimental profiles with theoretically computed profiles. Further, the modulator characteristics at the fundamental frequency (100 kHz) are known, but at third harmonic they are not known, since the pressure required at $k_0 = 0{\cdot}4312$ and drive frequency of 300 kHz would have been too high for the modulator to have retained its integrity.

Considering the piezoelectric transducer in the modulator as a forced damped vibrator (Chaudhary 1977), the phase of the output pressure pulse generated by the transducer will depend on its damping factor and its undamped natural frequency (along with the input frequency). This shows that, when a fundamental and a third harmonic are fed with a certain phase angle between them, the disturbance components generated are not necessarily at the same phase angle at the nozzle exit. This further complicates the comparison between experimental and theoretical jet profiles.

Many computer runs were made to achieve theoretical jet profiles similar to the various experimental profiles mentioned above. It was not possible to achieve exactly similar theoretical profiles in the neighbourhood of breakup. The reason for this discrepancy is not completely obvious. However, it is suspected that perhaps the effect of the initial velocity distribution is predominant, while in the theoretical solution a uniform velocity distribution was assumed.

A second objective was to adjust parameters so that the computed jet profiles corresponded as closely as possible to the 'carrot' shape mentioned earlier. Some of these results are shown in figures 5 and 6 of Chaudhary & Redekopp (1980). There we show that with sufficiently high harmonic input the theoretical profile does develop to a carrot shape and that the satellites can be eliminated as observed in the experiments.

REFERENCES

CHAUDHARY, K. C. 1977 Ph.D. thesis, University of Southern California.
CHAUDHARY, K. C. & MAXWORTHY, T. 1980 *J. Fluid Mech.* **86**, 275.
CHAUDHARY, K. C. & REDEKOPP, L. G. 1980 *J. Fluid Mech.* **96**, 257.
DONNELLY, R. J. & GLABERSON, W. 1966 *Proc. Roy. Soc.* A **290**, 547.
GOEDDE, E. F. & YUEN, M. C. 1970 *J. Fluid Mech.* **40**, 495.
HERZENBERG, L. A., SWEET, R. G. & HERZENBERG, L. A. 1976 *Sci. Amer.* **234**, 108.
RUTHLAND, D. F. & JAMESON, G. J. 1970 *Engng Sci.* **25**, 1689.
SWEET, R. G. 1964 *Stanford University Tech. Rep.* no. 1722–1.
YUEN, M. C. 1968 *J. Fluid Mech.* **32**, 15

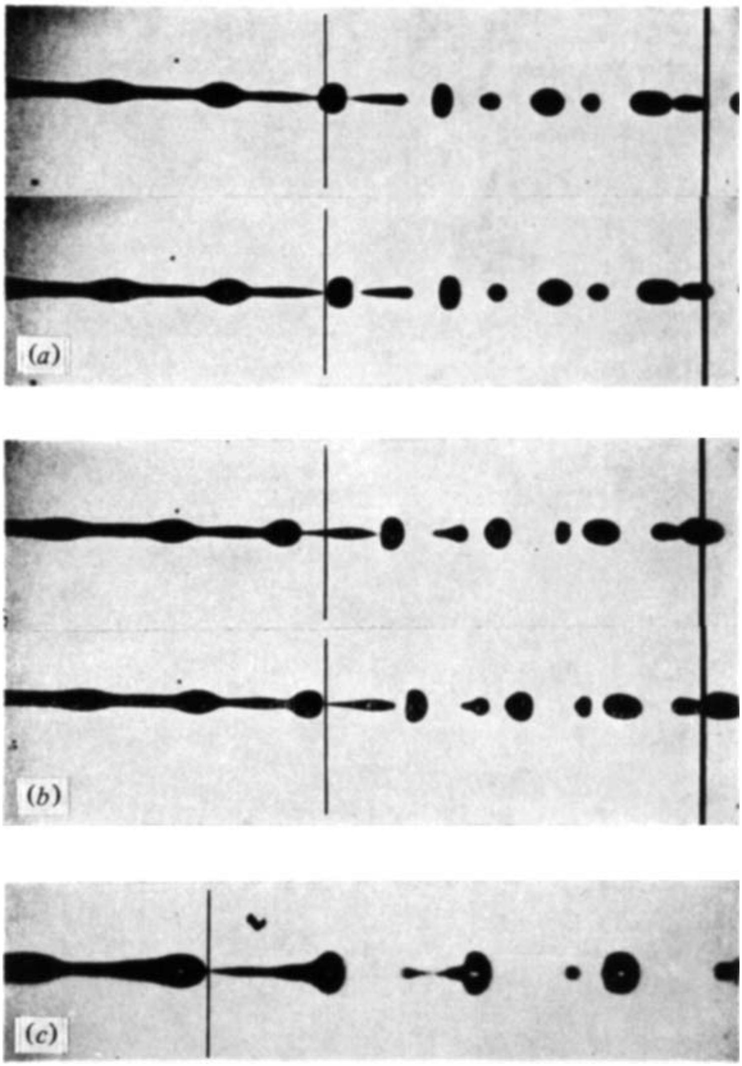

FIGURE 2. Typical ways of satellite formation: (*a*) forward separation and rear merging; in this case one wavelength of the fluid does not detach as one unit, hence it is not an acceptable configuration; (*b*) rear separation and forward merging; here again one wavelength of fluid does not detach as one unit, hence it is not an acceptable configuration; (*c*) rear separation and forward merging; here one wavelength of the fluid detaches as one unit and the satellite merges with the parent drop and hence it is an acceptable configuration.

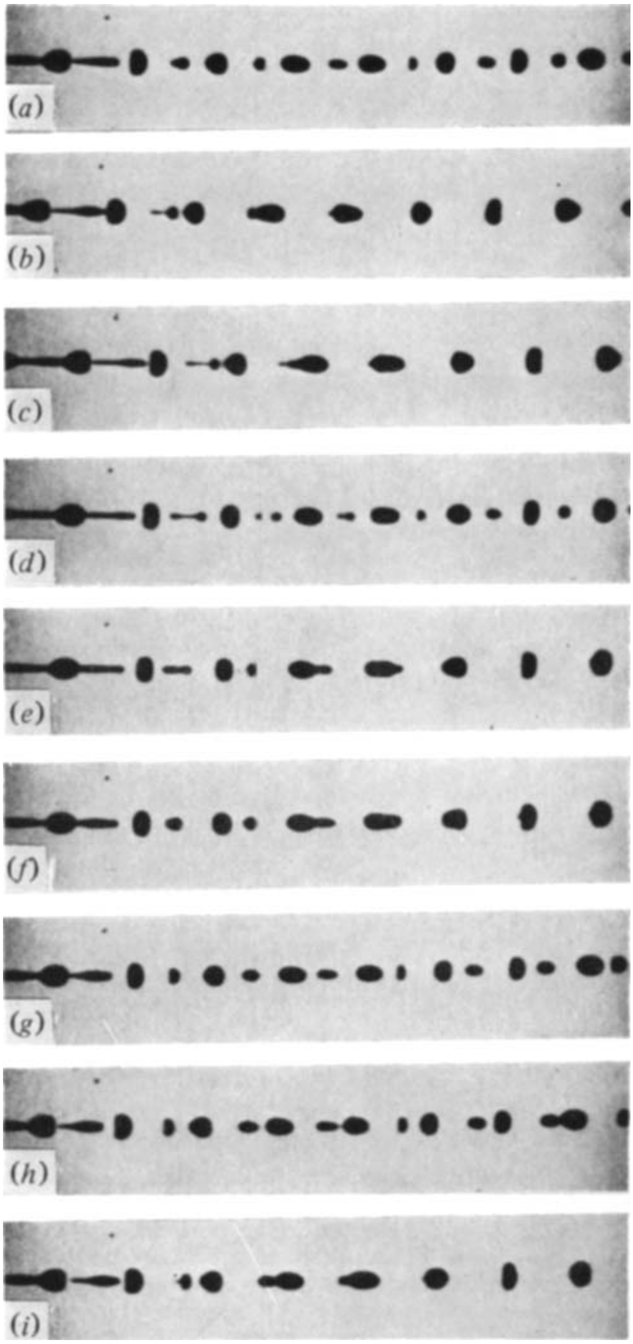

FIGURE 5. Control of direction of satellite merging with phase (θ) of the third harmonic. As θ is changed over 360°, the direction of the satellite merging changes by one cycle. $k_0 = 0{\cdot}4312$, $V_e = 8{\cdot}8$ V (r.m.s.), and $V_n = 2{\cdot}2$ V [except for (*a*) where $V_n = 0$]. (*b*) $\theta = 0°$, forward merge in 2 wavelengths; (*c*) $\theta = -45°$, forward merge in 3 wavelengths; (*d*) $\theta = -90°$, rear merge in 20 wavelengths; (*e*) $\theta = -135°$, rear merge in 3 wavelengths; (*f*) $\theta = -180°$, rear merge in 3 wavelengths; (*g*) $\theta = -225°$, rear merge in 17 wavelengths; (*h*) $\theta = -270°$, forward merge in 9 wavelengths; (*i*) $\theta = -315°$, forward merge in 3 wavelengths.

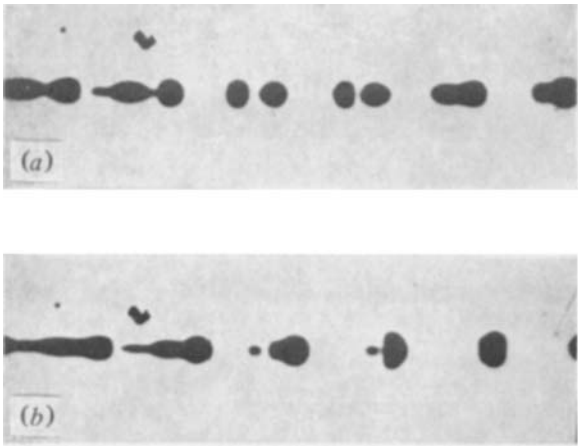

FIGURE 7. Two different patterns of satellite formation in the neighbourhood of the discontinuity shown in figure 6. (*a*) Fundamental: V_e = 18·5 V (r.m.s.); harmonic: V_n = 28 V (r.m.s.), $\theta = 0$. A satellite forms by pinching off the neck between it and the main drop, while the thin ligament behind the satellite coalesces with it. (*b*) Fundamental: V_e = 20 V (r.m.s.); harmonic: V_n = 16 V (r.m.s.), $\theta = 0°$. A small satellite forms by pinching off the thin rear ligament while the neck behind the main crest does not pinch off.

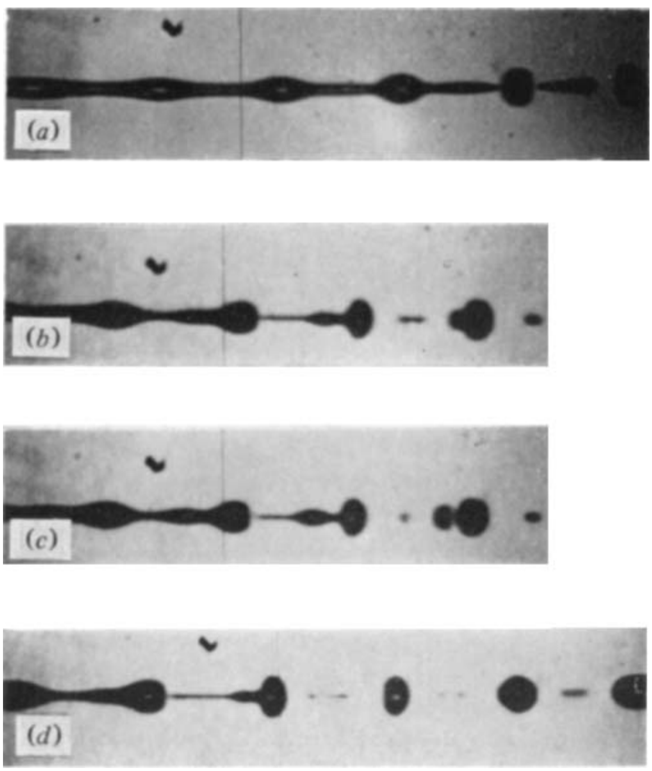

FIGURE 8. Satellite control with the third harmonic. k_0 = 0·4312 (the best wavenumber for control by the third harmonic). Low fundamental input, V_e = 3·5 V (r.m.s.); V_n = 3·5 V (r.m.s.) [except for (*a*) which is for $V_n = 0$]. (*a*) Unacceptable configuration; (*b*) $\theta = 0°$, acceptable configuration; (*c*) $\theta = +45°$, acceptable configuration; (*d*) $\theta = -45°$, acceptable configuration.

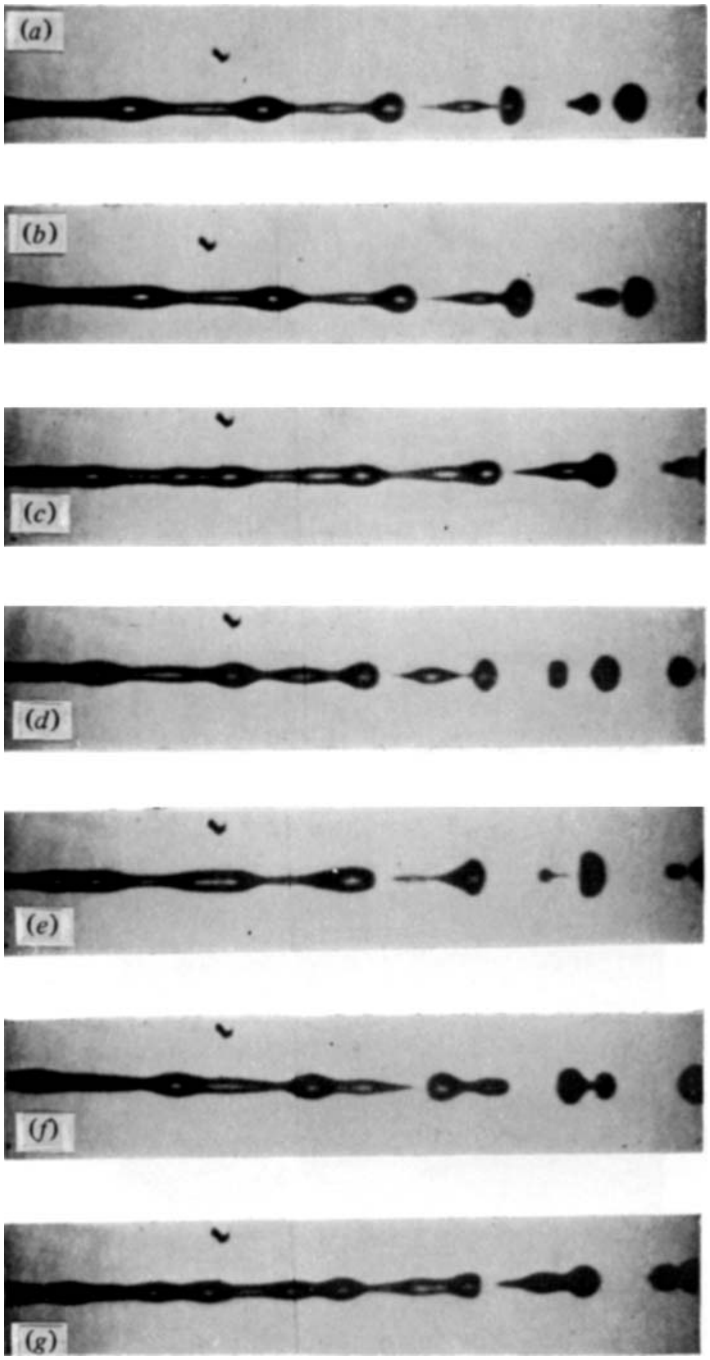

FIGURE 9. Satellite control with the third harmonic. $k_0 = 0{\cdot}4312$ and a fundamental input slightly less than the discontinuity point in figure 6. Fundamental: $V_e = 17{\cdot}7$ V (r.m.s.) for all cases. Harmonic varies: (*a*) $V_n = 0$ V, acceptable configuration; (*b*) $V_n = 1{\cdot}8$ V (r.m.s.), $\theta = 0°$, acceptable configuration; (*c*) $V_n = 8{\cdot}8$ V (r.m.s.), $\theta = 0°$, no satellites; (*d*) $V_n = 8{\cdot}8$ V (r.m.s.), $\theta = +90°$, acceptable configuration; (*e*) $V_n = 8{\cdot}8$ V (r.m.s.), $\theta = -135°$, acceptable configuration; (*f*) 8·8 V (r.m.s.), $\theta = 180°$, reverse formation, no satellites; (*g*) $V_n = 17{\cdot}7$ V (r.m.s.), $\theta = 0°$, no satellites.

CHAUDHARY AND MAXWORTHY

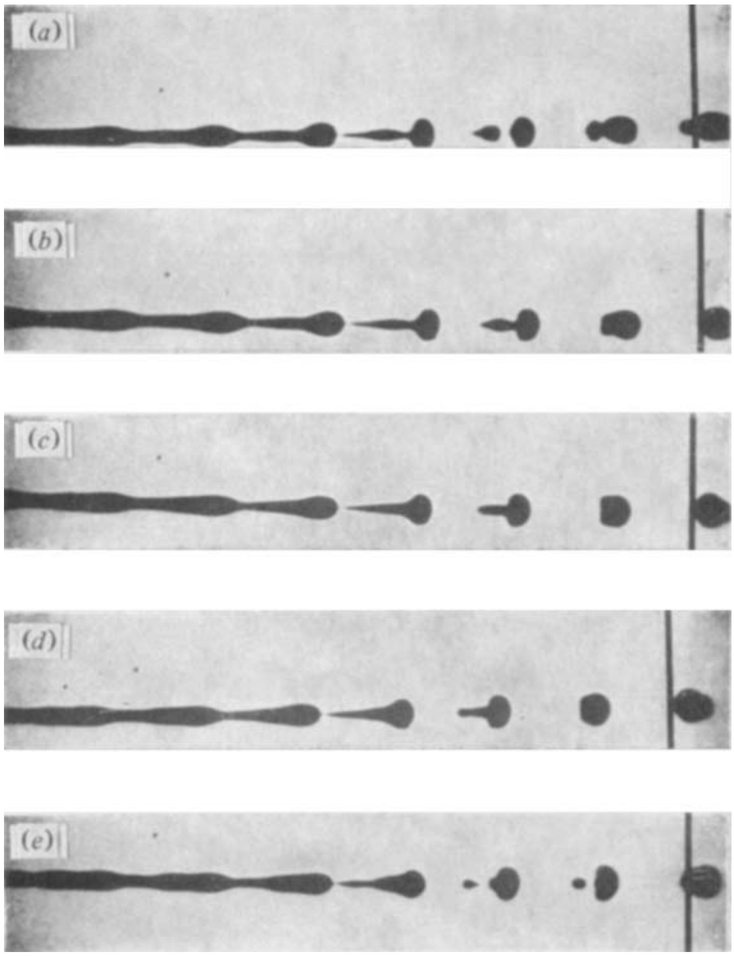

FIGURE 10. Satellite control with the third harmonic. $k_0 = 0{\cdot}4312$; $V_e = 30$ V (r.m.s.); all configurations are acceptable. Harmonic varies: (*a*) $V_n = 0$; (*b*) $V_n = 2$ V (r.m.s.), $\theta = 0°$; (*c*) $V_n = 5$ V (r.m.s.), $\theta = 0°$; (*d*) (*d*) $V_n = 7$ V (r.m.s.), $\theta = 0°$; (*e*) $V_n = 17$ V (r.m.s.), $\theta = 0°$.

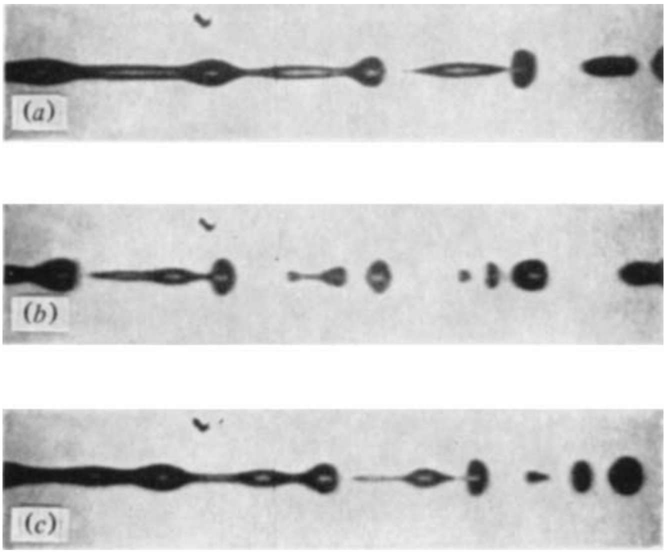

FIGURE 11. Satellite control with the third harmonic. $k_0 = 0{\cdot}335$ (very long wavelength). Requires fairly high fundamental input, but small harmonic input for acceptable configuration. Fundamental input $V_e = 28{\cdot}3$ V (r.m.s.). Harmonic input varies: (*a*) $V_n = 0$, unacceptable configuration; (*b*) $V_n = 1{\cdot}5$ V (r.m.s.), $\theta = 0°$, acceptable configuration; (*c*) $V_n = 2{\cdot}3$ V (r.m.s.), $\theta = 0°$, acceptable configuration.

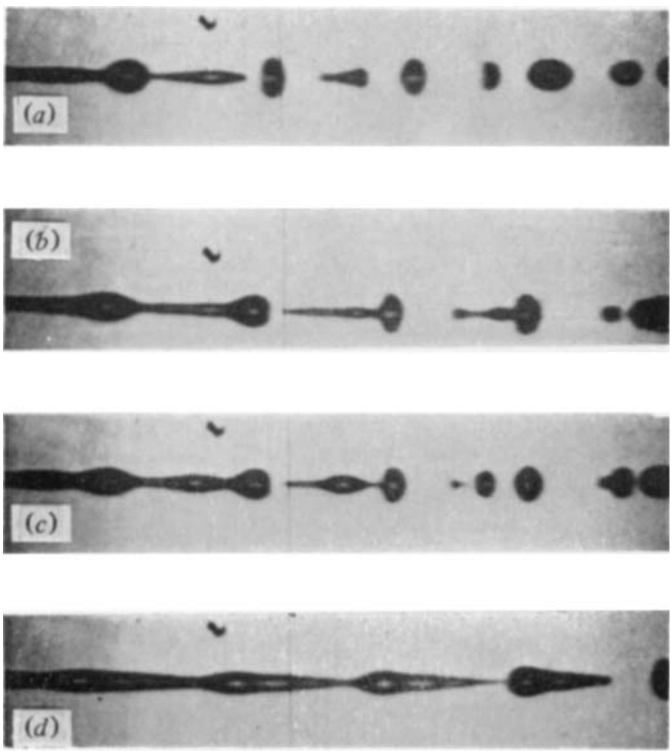

FIGURE 12. Satellite control with the third harmonic: effect of changing the phase of the harmonic. $k_0 = 0{\cdot}377$. Fundamental input $V_e = 8{\cdot}8$ V (r.m.s.). Harmonic input varies (*a*) $V_n = 0$, unacceptable configuration; (*b*) $V_n = 1{\cdot}8$ V (r.m.s.), $\theta = 0°$, acceptable configuration; (*c*) $V_n = 3{\cdot}5$ V (r.m.s.), $\theta = +90°$, acceptable configuration; (*d*) $V_n = 3{\cdot}5$ V (r.m.s.), $\theta = -90°$, reverse formation in comparison to figure (*c*), acceptable configuration.

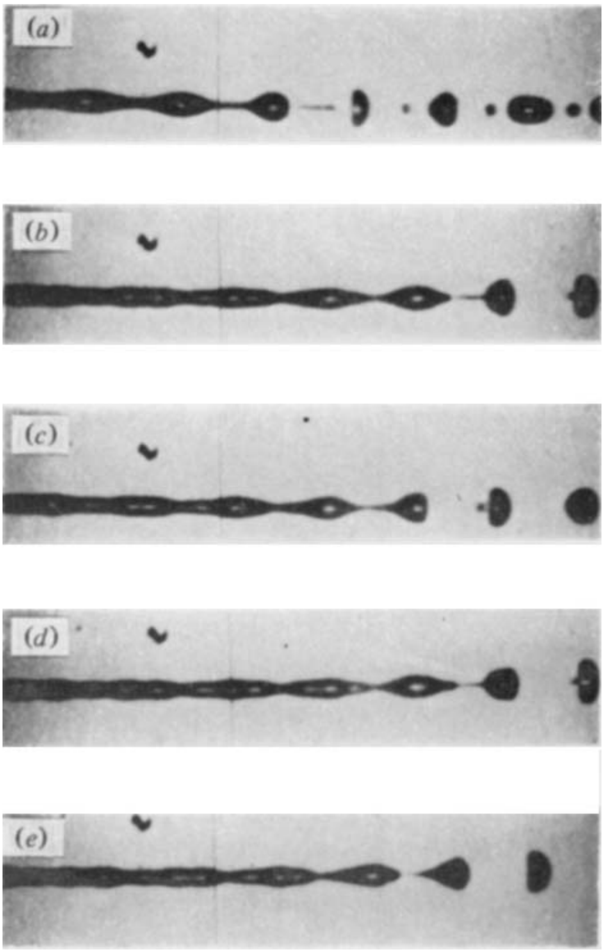

FIGURE 13. Satellite control with the third harmonic. $k_0 = 0{\cdot}604$, short wavelength. Fundamental input $V_e = 17{\cdot}7$ V (r.m.s.). Harmonic input varies: (*a*) $V_n = 0$, unacceptable configuration; (*b*) $V_n = 12{\cdot}4$ V (r.m.s.), $\theta = 0°$; (*c*) $V_n = 12{\cdot}4$ V (r.m.s.), $\theta = -135°$, acceptable configuration; (*d*) $V_n = 17{\cdot}7$ V (r.m.s.), $\theta = -225°$, no satellites; (*e*) $V_n = 17{\cdot}7$ V (r.m.s.), $\theta = +90°$, no satellites, preferred configuration compared to above because of smaller thin ligament.

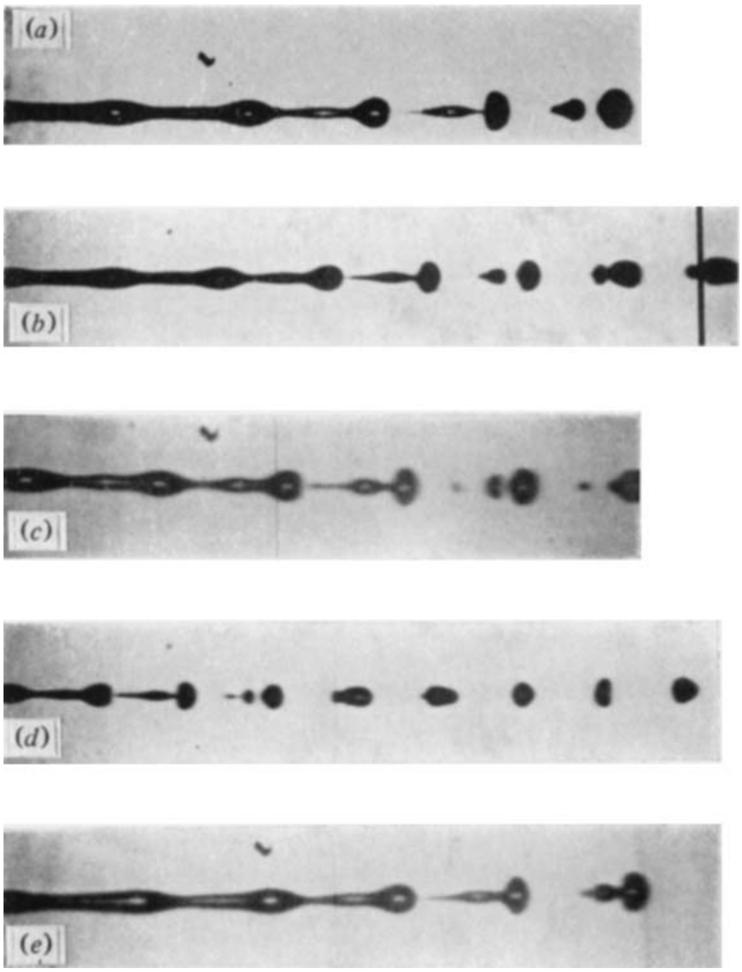

FIGURE 14. Comparison of jet profiles at various input values with and without third harmonic input. $k_0 = 0{\cdot}4312$, $\theta = 0°$. (*a*) $V_e = 17{\cdot}7$ V (r.m.s), $V_n = 0$; (*b*) $V_e = 30$ V (r.m.s.), $V_n = 0$; (*c*) $V_e = 3{\cdot}5$ V (r.m.s.), $V_n = 3{\cdot}5$ N (r.m.s.); (*d*) $V_e = 8{\cdot}8$ V (r.m.s.), $V_n = 3{\cdot}5$ V (r.m.s.); (*e*) $V_e = 8{\cdot}8$ V (r.m.s.), $V_n = 3{\cdot}5$ V (r.m.s.).

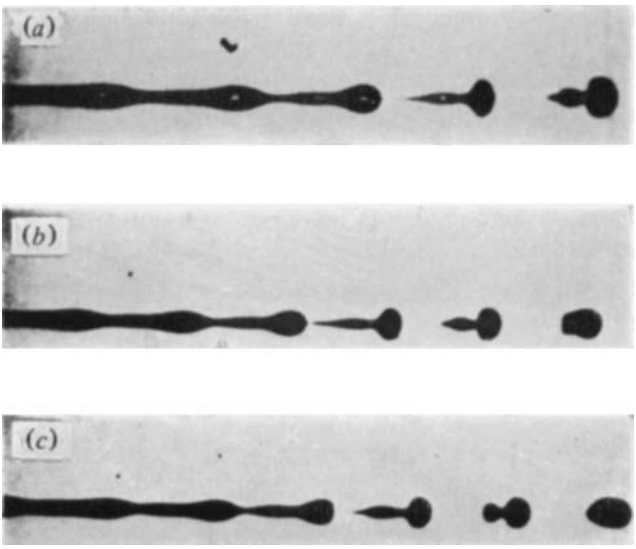

FIGURE 15. Comparison of jet profiles at various input values for the fundamental and third harmonic. $k_0 = 0{\cdot}4312$, $\theta = 0°$. (*a*) $V_e = 8{\cdot}6$ V (r.m.s.), $V_n = 3{\cdot}5$ V (r.m.s.); (*b*) $V_e = 30$ V (r.m.s.), $V_n = 2$ V (r.m.s.); (*c*) $V_e = 50$ V (r.m.s.), $V_n = 1$ V (r.m.s.).

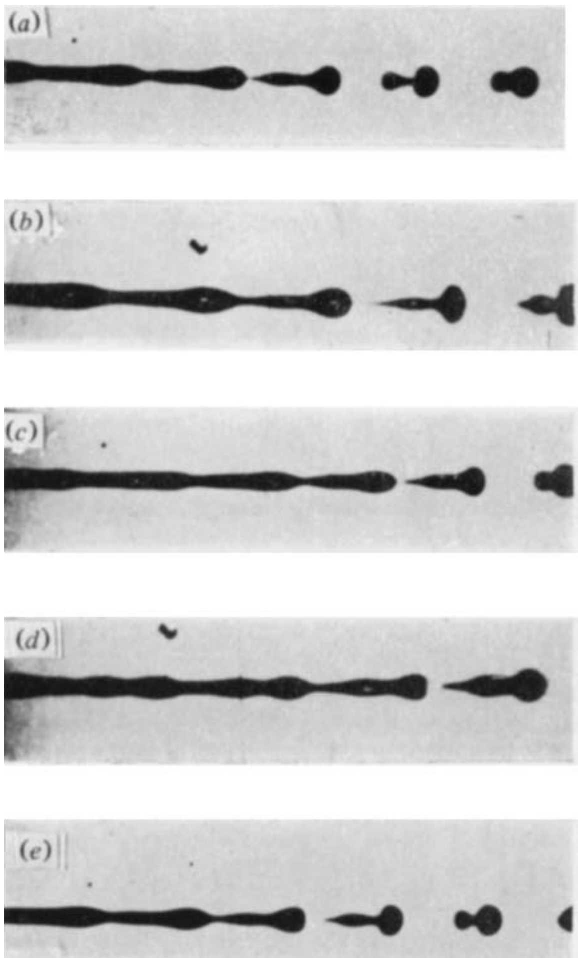

FIGURE 16. Comparison of jet profiles at various input values for the fundamental, with and without the third harmonic. $k_0 = 0{\cdot}4312$, $\theta = 0°$. (*a*) $V_e = 70$ V (r.m.s.), $V_n = 0$; (*b*) $V_e = 8{\cdot}8$ V (r.m.s.), $V_n = 3{\cdot}5$ V (r.m.s.); (*c*) $V_e = 8{\cdot}8$ V (r.m.s.), $V_n = 8{\cdot}8$ V (r.m.s.); (*d*) $V_e = 17{\cdot}7$ V (r.m.s.), $V_n = 17{\cdot}7$ V (r.m.s.); (*e*) 50 V (r.m.s.), $V_n = 1$ V (r.m.s.).